ISSN 1063-7834, Physics of the Solid State, 2021, Vol. 63, No. 2, pp. 372–376. © Pleiades Publishing, Ltd., 2021.
Russian Text © The Author(s), 2021, published in Fizika Tverdogo Tela, 2021, Vol. 63, No. 2, pp. 308–312.

THERMAL PROPERTIES

Electronic and Thermophysical Properties of Gas Hydrates: Ab Initio Simulation Results

M. B. Yunusov[a, *], R. M. Khusnutdinoff[a, b], and A. V. Mokshin[a, b]

[a] *Kazan Federal University, Kazan, 420008 Russia*

[b] *Udmurt Federal Research Center, Ural Branch, Russian Academy of Sciences, Izhevsk, 426067 Russia*

**e-mail: mukhammadbek@mail.ru*

Received September 23, 2020; revised October 2, 2020; accepted October 2, 2020

Abstract—Results of ab initio molecular-dynamic investigation of the electronic and thermophysical properties of methane hydrate with cubic structure sI are represented. The simulation results for specific heat at constant volume and density are in good agreement with experimental data. The temperature dependences of the electronic properties of methane hydrate (including Fermi energy level and width and edges of the band gap) are determined based on analysis of the density of electronic states. For an empty hydrate framework (aqueous clathrate framework), the spectra of electron energy $E(\mathbf{k})$ along the M–X, X–Γ, Γ–M, and Γ–R directions are calculated. It is established that the presence of CH_4 molecules in the aqueous clathrate increases the hydrate Fermi energy from 2.4 to 3.0 eV.

Keywords: ab initio calculations, density of electronic states

DOI: 10.1134/S1063783421020268

1. INTRODUCTION

Natural hydrates are a form of existence of gas in Earth interior and promising sources of hydrocarbon gas [1]. Hydrates of natural gases (or gas hydrates) are nonstoichiometric compounds, in which incorporated gas molecules (guest molecules) are enclosed in cavities of a three-dimensional lattice of water molecules (host framework). The stability of aqueous clathrate frameworks (which are thermodynamically less stable than ice or liquid water under the same conditions) is provided by van der Waals guest–host interactions [1–8]. For example, stabilization of the gas-hydrate structure is due to repulsion of the water framework from inner gas molecules. In [9], the structural stability and electronic properties of different gas hydrates (CO_2, CO, CH_4, and H_2) were thoroughly investigated using quantum-mechanical simulation within the generalized gradient approximation. It was shown that filling of an aqueous clathrate framework with a gas (CO_2, CO, CH_4, or H_2) increases the stability of the hydrate structure. It was established that carbon dioxide hydrate is most stable in comparison with the other gas hydrates (its binding energy was –2.36 eV). Hydrogen hydrate was least stable (binding energy –0.36 eV). The methane hydrate (binding energy was –0.58 eV).

The structure types of most popular gas hydrates are cubic structures I and II and hexagonal structure III (denoted as sI, sII, and sIII, respectively) [2]. Methane hydrate is mainly crystallized into the cubic structure (known as type sI), in which both large water clusters (with a diameter of 5.86 Å) and small water clusters (with a diameter of ~5.10 Å) can capture a methane molecule, the diameter of which is ~4.36 Å [10, 11]. This system is generally formed when methane and water are brought into contact at room temperature (i.e., $T \sim 300$ K) and a moderate pressure ($p \geq 0.6$ MPa) [12]. Currently, structural features and thermophysical properties of gas hydrates are of great interest for researchers because of the following factors. First, natural-gas hydrates can be used as a new source of hydrocarbon fuel. According to estimates, reserves of gas in hydrates are $\sim 2 \times 10^{16}$ m^3, which several orders of magnitude higher than reserves of conventional natural gas [1, 2]. Second, the problem of hydrate-formation in wellbores and gas pipelines is very urgent in gas industry.

The purpose of this study was to perform ab initio investigation of the electronic and thermophysical properties of gas hydrates with characteristic cubic structure sI.

2. DETAILS OF CALCULATIONS

Large-scale ab initio molecular-dynamic studies of methane hydrate with cubic structure sI were carried out in the VASP software package [13, 14]. The crystal structure of clathrate hydrate sI was generated based on X-ray diffraction data obtained by Stackelberg and Müeller [15] and Pauling and Marsh [16] and the algo-

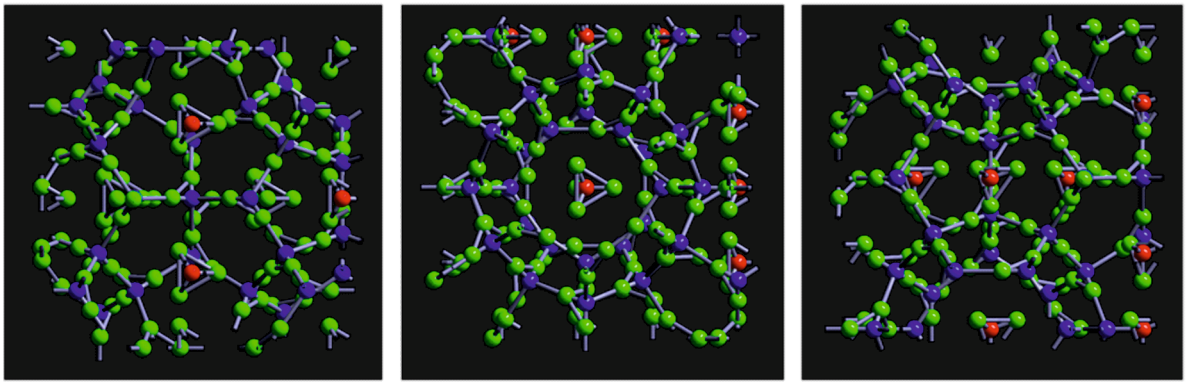

Fig. 1. Methane hydrate cell with structure sI in three projections: carbon, oxygen, and hydrogen atoms are shown red, blue, and green, respectively. Colored in the online version.

rithm of optimization of hydrogen atomic positions using the Bernal–Fowler rules, taking into account zero total dipole moment. Methane hydrate is formed via incorporation of CH_4 molecules into free cavities of the aqueous clathrate framework. The simulated system was 12 × 12 × 12 Å in size and included eight methane molecules (it consisted of 178 hydrogen, carbon, and oxygen ions). Figure 1 shows a methane hydrate cell with structure sI in three projections. The simulation was performed in an isothermal–isochoric NVT ensemble for the temperature range T = [200; 300] K with temperature step ΔT = 20 K. The thermodynamic equilibrium state was established using the Nose–Hoover thermostat. To avoid undesirable surface phenomena and the finite-dimensional system effect, periodic boundary conditions were imposed on the simulation cell in all directions. The basis set consisted of plane waves; the electron–ion interaction was performed using ultrasoft smoothed pseudopotentials; and the exchange-correlation energy was calculated within the generalized gradient approximation [13, 14].

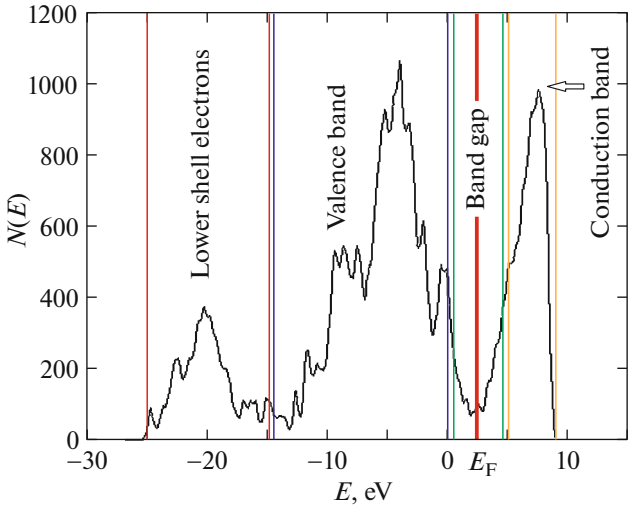

Fig. 2. Density of electronic states and energy bands for methane hydrate with cubic structure sI at T = 200 K. Colored in the online version.

3. RESULTS AND DISCUSSION

To check the correctness of the simulation results, we calculated the mass density of crystalline methane hydrate. The obtained value for the system under study was ρ = 918.4 kg/m^3, which is in good agreement with the experimental value of ρ = 910.0 kg/m^3 [17]. The temperature dependence of the total system energy was calculated for the range T = [200; 300] K; this dependence was found to be approximated well by the linear dependence

$$E(T) = 3.748\times10^{-21}T + 1.374\times10^{-16}\ \text{(J)}. \qquad (1)$$

The average specific heat at a constant volume was calculated from the formula

$$C_V = \frac{1}{m}\frac{dQ}{dT} = \frac{1}{m}\left(\frac{dE}{dT} + p\frac{dV}{dT} - \mu\frac{dN}{dT}\right) = \frac{1}{m}\frac{dE}{dT}. \qquad (2)$$

The obtained specific heat value was C_v = 2362.5 J/(kg K), which is in good agreement with the experimental data (C_v = 2160 ± 100 J/(kg K) [18] and 2306 J/(kg K) [19]). For the system under study, the density of electronic states $N(E)$ was calculated at temperatures from the range T = [200; 300] K with step ΔT = 20 K. The density of electronic states and energy bands for the gas hydrate with cubic structure sI at T = 200 K are presented in Fig. 2. The calculated dependences $N(E)$ are in good qualitative agreement with the results of quantum-mechanical calculations for different gas hydrates (CO_2, CO, CH_4, and H_2)[1] [9]. To determine the band gap edges, we performed the procedure of fitting spectral line shapes by Gaussian

[1] In [9], the Fermi level is shifted to the left along the horizontal axis, i.e., E_F = 0 eV.

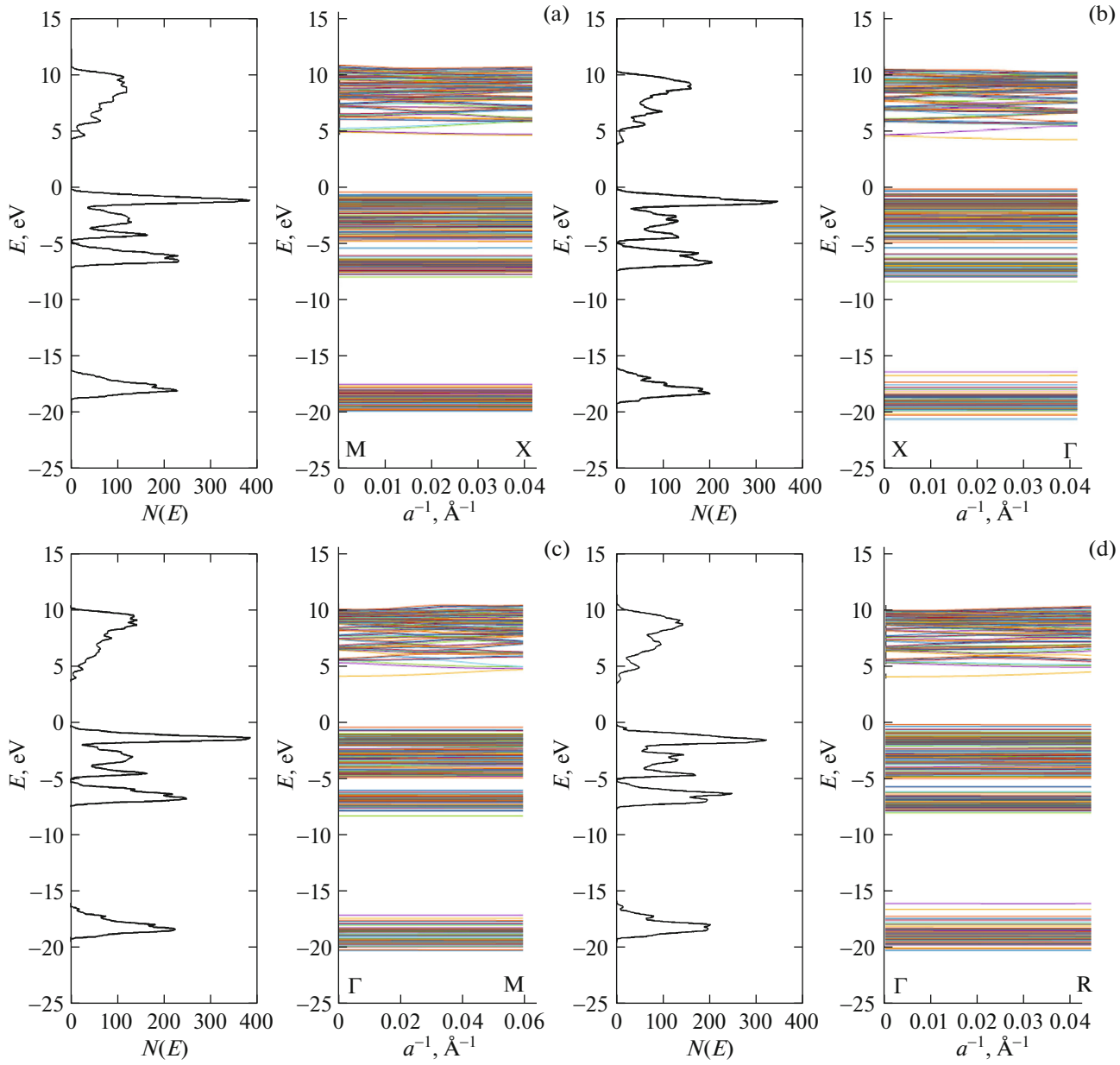

Fig. 3. Density of electronic states and electron energy spectrum $E(\mathbf{k})$ along the directions: (a) M–X, (b) X–Γ, (c) Γ–M, and (d) Γ–R. The abscissa axis for the dependence $E(\mathbf{k})$ is normalized to quantity a^{-1}, where a is the lattice parameter ($a = 12$ Å). Colored in the online version.

functions. Approximation of the peaks of the density of electronic states adjacent to the band gap made it possible to determine approximate values of the energies of the top of the valence band ($E_{G\max}$) and bottom of the conduction band ($E_{G\min}$). The position of the Fermi level was determined as

$$E_{\mathrm{F}} = \frac{E_{G\max} + E_{G\min}}{2} + \frac{3}{4} k_{\mathrm{B}} T \ln\left(\frac{m_p}{m_n}\right), \qquad (3)$$

where m_p and m_n are the effective hole and electron masses [20]. Due to the smallness of the addend in (3), this contribution was disregarded in the calculation of the Fermi level positions. The obtained values for the width (ΔE_G) and edges ($E_{G\max}$ and $E_{G\min}$) of the band gap and Fermi energy E_{F} for methane hydrate with cubic structure sI are listed in Table 1.

As can be seen, the Fermi level is located (with a high accuracy) in the middle of the band gap. The obtained values of the band gap ΔE_G between the bottom of the conduction band and the top of the valence band are in good agreement with the results of quantum-mechanical calculations for methane hydrate

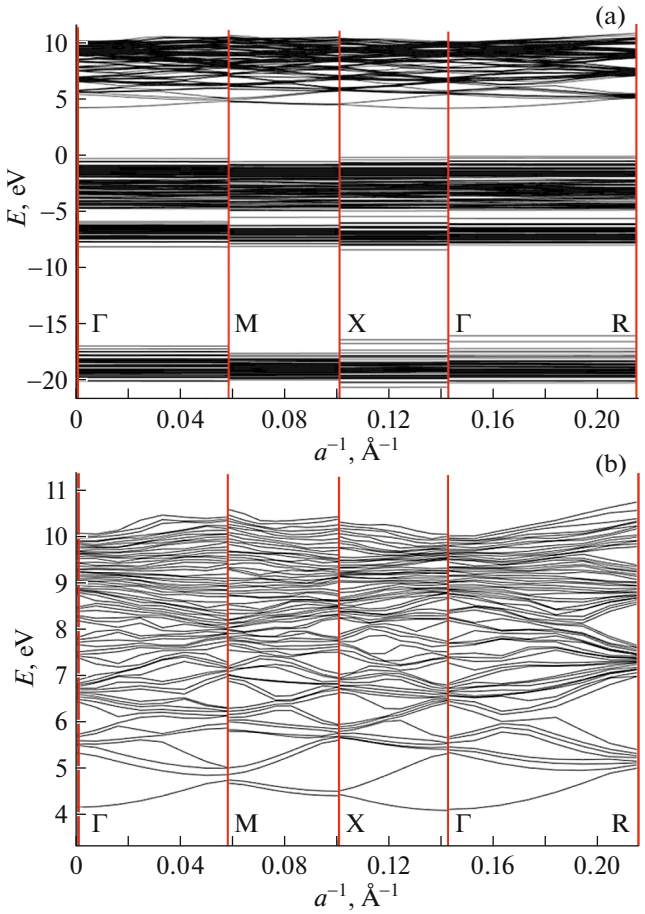

Fig. 4. (a) Energy band structure of the hydrate crystal with cubic structure sI with empty molecular cavities. (b) Conduction band on an enlarged scale. Colored in the online version.

with cubic structure sI at three different configurations [21] denoted as cI, cII, and cIII. The ΔE_G values for methane hydrate with configurations cI, cII, and cIII were 5.27, 5.23, and 3.81 eV, respectively.

In addition, an increase in the energies of the top and bottom of the band gap with an increase in temperature was found for the system under study. Linear approximation of the Fermi energy values was performed in the temperature range of 200–300 K. With an increase in temperature, the bottom of the conduction band is lifted with average rate $dE_{G\max}/dT$ = 0.0053 eV/K. The top of the valence band is lifted with average rate $dE_{G\min}/dT$ = 0.0035 eV/K. The Fermi energy increases with rate dE_F/dT = 0.0044 eV/K. The difference in the increase rates of the edges of the band gap leads to a change in its width. Its average expansion rate was dE_G/dT = 0.0018 eV/K.

For the hydrate sI framework with empty molecular cavities, the energy band structure was calculated, which is a dependence of the electron energies on wave vector $E(\mathbf{k})$ and gives an idea of the character of change in the electron energy during the motion along some direction in the wave-vector space. Since the electron energy in a crystal is a periodic function on $\mathbf{k}$, one can consider only the wave vector $\mathbf{k}$ from the range $-\pi/a < k < \pi/a$ (i.e., only the first Brillouin zone) when studying the electron energy spectrum. The lines connecting high-symmetry points are generally considered as preferential directions of the wave vector. Hydrate sI is characterized by a cubic lattice, for which the Brillouin zone has a cubic shape. Figure 3 shows the density of electronic states and the electron energy spectrum $E(\mathbf{k})$ for the hydrate sI framework with empty molecular cavities along the M–X, X–Γ, Γ–M, and Γ–R directions (here, Γ, X, M, and R are the center of the Brillouin zone, center of the face, center of the edge, and vertex, respectively).

Figure 4 shows the energy band structure of the hydrate crystal with cubic structure sI with empty molecular cavities. It can be seen that electrons from the lower energy levels (−20 to −17 eV) and valence band (−8 to 0 eV) have (with a high accuracy) linear dependence $E(\mathbf{k})$. Spectrum $E(\mathbf{k})$ in the energy range of 5–10 eV (which corresponds to the conduction band) has local maxima and minima at points Γ, M, X, and R. The top and bottom of the conduction band have maxima at point R and minima at point Γ. The band gap in the hydrate sI crystal has width $\Delta E_G \approx$ 5.0 eV. The Fermi energy is $E_F \approx$ 2.4 eV, which is smaller than the value for hydrate sI with inclusions in methane molecule cavities ($E_F \approx$ 3.0 eV).

Table 1. Temperature dependences of width (ΔE_G) and edges ($E_{G\max}$ and $E_{G\min}$) of the band gap and Fermi energy E_F for methane hydrate with cubic structure sI

T, K	$E_{G\max}$, eV	$E_{G\min}$, eV	E_F, eV	ΔE_G, eV
200	4.895	1.257	3.076	3.638
220	4.897	1.091	3.039	3.896
240	4.979	1.066	3.023	3.912
260	5.090	1.471	3.281	3.620
280	5.148	1.332	3.240	3.816
300	5.310	1.302	3.306	4.009

4. CONCLUSIONS

We presented the results of large-scale ab initio simulation of methane hydrate with cubic structure sI for a wide temperature range. The simulation results for the density and specific heat at a constant volume were found to be in good agreement with the experimental data [17–19]. Temperature dependences of the electronic properties of methane hydrate (Fermi energy and width and edges of the band gap) were determined based on analysis of the density of electronic states. It was established that the bottom of the conduction band and the top of the valence band are

lifted with an increase in temperature with average rates $dE_{G\max}/dT = 0.0053$ eV/K and $dE_{G\min}/dT = 0.0035$ eV/K, respectively. At the same time, the Fermi level increase rate was $dE_F/dT = 0.0044$ eV/K. The electron energy spectrum $E(\mathbf{k})$ was calculated along the M–X, X–Γ, Γ–M, and Γ–R directions for a hydrate crystal with cubic structure sI with empty molecular cavities. It was established that the presence of methane molecules leads to an increase in the hydrate Fermi energy from 2.4 to 3.0 eV.

ACKNOWLEDGMENTS

Large-scale molecular-dynamics calculations were performed on the equipment of the Shared Research Center for High-Performance Computing of the Moscow State University and the Computational Cluster of the Kazan Federal University.

FUNDING

This study was supported by the Russian Science Foundation (project no. 19-12-00022).

CONFLICT OF INTEREST

The authors declare that they have no conflicts of interest.

REFERENCES

1. E. D. Sloan and C. A. Koh, *Clathrate Hydrates of Natural Gases*, 3rd ed. (CRC, Taylor and Francis, USA, 2007).
2. N. J. English and J. M. D. MacElroy, Chem. Eng. Sci. **121**, 133 (2015).
3. R. M. Khusnutdinoff and A. V. Mokshin, J. Non-Cryst. Solids **357**, 1677 (2011).
4. R. M. Khusnutdinoff and A. V. Mokshin, Phys. A (Amsterdam, Neth.) **391**, 2842 (2012).
5. R. M. Khusnutdinov, Colloid J. **75**, 726 (2013).
6. R. M. Khusnutdinoff and A. V. Mokshin, J. Cryst. Growth **524**, 125182 (2019).
7. R. M. Khusnutdinov and A. V. Mokshin, JETP Lett. **110**, 557 (2019).
8. R. M. Khusnutdinoff and A. V. Mokshin, Phys. Solid State **62**, 869 (2020).
9. P. Guo, Y.-L. Qiu, L.-L. Li, Q. Luo, J.-F. Zhao, and Y.-K. Pan, Chin. Phys. B **27**, 043103 (2018).
10. I.-M. Chou, A. Sharma, R. C. Burruss, J. Shu, H.-K. Mao, R. J. Hemley, A. F. Goncharov, L. A. Stern, and S. H. Kirby, Proc. Natl. Acad. Sci. U. S. A. **97**, 13484 (2000).
11. M. Ota, K. Morohashi, Y. Abe, M. Watanabe, J. R. L. Smith, and H. Inomata, Energy Convers. Manag. **46**, 1680 (2005).
12. M. E. Casco, J. Silvestre-Albero, A. J. Ramirez-Cuesta, F. Rey, J. L. Jorda, A. Bansode, A. Urakawa, I. Peral, M. Martínez-Escandell, K. Kaneko, and F. Rodríguez-Reinoso, Nat. Commun. **6**, 6432 (2015).
13. G. Kresse and J. Hafner, Phys. Rev. B **47**, 558 (1993).
14. G. Kresse and J. Furthmuller, Phys. Rev. B **54**, 11169 (1996).
15. M. Stackelberg and H. R. Müller, Z. Elktrochem. **58**, 25 (1954).
16. L. Pauling and R. E. Marsh, Proc. Natl. Acad. Sci. U. S. A. **38**, 112 (1952).
17. Yu. F. Makogon, Geol. Polez. Iskop. Mirov. Okeana, No. 2, 5 (2010).
18. W. F. Waite, L. A. Stern, S. H. Kirby, W. J. Winters, and D. H. Mason, Geophys. J. Int. **169**, 767 (2007).
19. V. I. Istomin and V. S. Yakushev, *Natural Gas Hydrates* (Nedra, Moscow, 1992) [in Russian].
20. N. Ashcroft and N. Mermin, *Solid State Physics* (Brooks Cole, Pacific Grove, 1976).
21. Z. Wang, L. Yang, R. Deng, and Z. Yang, arXiv: 1902.10914v1 (2019).

Translated by A. Sin'kov